

Measurement of atomic diffraction phases induced by material gratings

John D. Perreault and Alexander D. Cronin

Department of Physics, University of Arizona, Tucson, Arizona 85721, USA

(Received 24 August 2005; published 15 March 2006)

Atom-surface interactions can significantly modify the intensity and phase of atom de Broglie waves diffracted by a silicon nitride grating. This affects the operation of a material grating as a coherent beam splitter. The phase shifts induced by diffraction are measured by comparing the relative phases of several interfering paths in a Mach-Zehnder Na atom interferometer formed by three material gratings. The values of the diffraction phases are consistent with a simple model which includes a van der Waals atom-surface interaction between the Na atoms and the silicon nitride grating bars.

DOI: [10.1103/PhysRevA.73.033610](https://doi.org/10.1103/PhysRevA.73.033610)

PACS number(s): 03.75.Be, 03.75.Dg, 34.20.Cf, 39.20.+q

A coherent beam splitter is a useful component for constructing an atom interferometer [1]. The purpose of the beam splitter is to generate a quantum superposition of atom waves, propagating along two paths which can be recombined to form an interference pattern. The contrast and phase of the interference pattern can then be used to study interactions that affect the atoms differently in the two interferometer paths. However, atom wave beam splitters formed using laser light [2–4] and material grating structures [5] can create beams with differing complex amplitudes. A familiar analogy of this in optics occurs for light beam splitters formed using glass plates, thin metal films, and multilayer dielectric stacks which all cause a phase shift between the reflected and transmitted components [6]. These complex amplitudes are an important concern when building an atom interferometer since they affect the phase and contrast of the interference pattern, and have been identified as a source of uncertainty for atom interferometer gyroscopes [7]. Here we present evidence of beam splitter induced phase shifts in an atom interferometer based on material gratings and a method for measuring these phase shifts for interferometers that utilize diffraction.

The van der Waals (vdW) atom-surface interaction [8] plays a significant role in determining the intensity and phase (diffraction phase) of atom waves split by a material grating. Several atom-optics experiments have observed how atom-surface interactions can affect the intensity of atom waves [5,9,10]. By comparison, only one experiment to our knowledge has directly measured the diffraction phase induced by atom-surface interactions, particularly for the zeroth order [11]. In this paper the first and second order diffraction phases are measured by comparing the phase difference between the various interfering paths in a three-grating Mach-Zehnder atom interferometer. The paths of the interferometer are formed using two *different* diffraction orders. Therefore, the relative phases of the paths are in part determined by the higher order diffraction phases, which must be understood in order to describe how the gratings operate as a beam splitter.

The experimental setup used to measure the atomic diffraction phases induced by a material grating is shown in Fig. 1. A Mach-Zehnder atom interferometer, similar to the one described in Ref. [12], is formed using diffraction from three 100 nm period silicon nitride gratings [13] which are denoted G_1, G_2 , and G_3 . These gratings are nominally sep-

rated by 1 m. A collimated supersonic Na atom beam is first diffracted by grating G_1 , inducing a phase shift which depends on the diffraction order and will be described later. Each diffracted beam then undergoes first order diffraction by G_2 and forms a spatial interference pattern just before G_3 . The atoms transmitted through G_3 are ionized by a 60 μm wide hot Re wire and counted by a channel electron multiplier. Grating G_3 is then scanned in the direction transverse to the incident atom beam (x axis) to determine the phase of the interference pattern. While there are many paths which can interfere at the plane of G_3 only the ones which involve first order diffraction by G_2 (as indicated in Fig. 1) will lead to a significant interference signal because of atom velocity dispersion and the use of G_3 as a transmission mask. Since each relevant path through G_2 undergoes first order diffraction both paths acquire the same diffraction phase, which means there is no net phase shift induced by G_2 . In addition, grating G_3 acts as a transmission mask so only the diffraction phases induced by G_1 will lead to a relative phase shift between the interfering paths. This treatment is appropriate for the present experiment since the detector is in the near-field of G_3 . In principle, the diffraction phases can then be determined by comparing the phase of the various spatially resolved interferometer outputs. The interferometer outputs were measured separately by moving the detector along the x axis, as shown in Fig. 2.

In practice there are two types of phase shifts that need to be considered when predicting the relative phase of the various interferometer outputs. One originates from the diffraction phase induced by G_1 and the other from a distance mismatch between the gratings G_1, G_2 , and G_3 , which is denoted by $\Delta L \equiv L'' - L'$ in Fig. 1. In order to report a measurement of the diffraction phases, expressions for both of these phase shifts will be put forth.

From previous work it has been shown that atomic diffraction from a material grating will create diffracted beams with complex amplitudes ψ_n given by

$$\psi_n = A_n e^{i\Phi_n} \propto \int_{-w/2}^{w/2} e^{i\phi(\xi)} e^{i2\pi\xi n/d} d\xi, \quad (1)$$

where A_n is the amplitude and Φ_n is the diffraction phase for a given diffraction order n as derived in [5,10,11]. The vari-

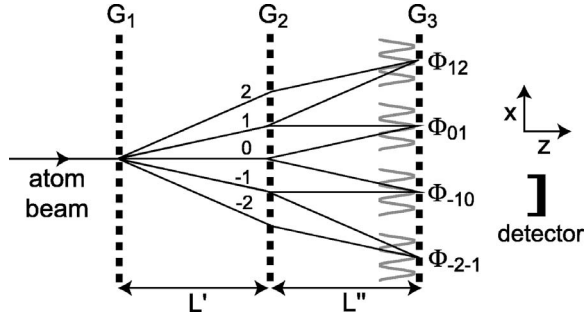


FIG. 1. Experimental setup for measuring diffraction phases with an atom interferometer formed by the three gratings G_1, G_2 , and G_3 . Since the interference pattern is read out using G_3 as a mask and the atoms have a velocity distribution, only the paths indicated by the solid lines will lead to a significant interference signal. The mismatch of the grating spacings $\Delta L \equiv L'' - L'$ and the diffraction phases Φ_n induced by G_1 determine the measured interference phases Φ_{mn} of the four spatially resolved outputs.

able ξ is the position measured from the center of the grating window whose size is w , and the grating period is d . The expression in Eq. (1) is valid in the far-field (Fraunhofer) diffraction regime and is appropriate for our experimental setup as described in [5]. The phase $\phi(\xi)$ represents the phase accumulated by the atom wave as it propagates through the grating window, given by the WKB approximation to leading order in $V(\xi)$ as

$$\phi(\xi) = -\frac{lV(\xi)}{\hbar v}, \quad (2)$$

where l is the thickness of the grating, \hbar is Planck's constant, and v is the atom beam velocity which can be related to the de Broglie wavelength $\lambda_{dB} = h/mv$ [5]. The atom-surface interaction potential $V(\xi)$ in Eq. (2) is given by

$$V(\xi) = -C_3 \left[\left| \xi - \frac{w}{2} \right|^{-3} + \left| \xi + \frac{w}{2} \right|^{-3} \right], \quad (3)$$

where C_3 is coefficient describing the strength of the vdW interaction. This form of the vdW potential is valid for atom-surface distances of $\lesssim 1 \mu\text{m}$ for ground-state Na atoms and neglects the finite thickness of the grating bars [5,8]. Plots of the diffraction phases and amplitudes are shown in Fig. 3 as a function of C_3 . From Eqs. (1) through (3) it is also clear that $\Phi_n = \Phi_{-n}$, since $\phi(-\xi) = \phi(\xi)$.

There is also a phase shift between the interferometer outputs induced by a distance mismatch of the gratings G_1, G_2 , and G_3 along the z axis. The origin of this phase shift can be understood by recalling that when two plane waves interfere at an angle $\theta = \lambda_{dB} d^{-1}$, interference fringes will be formed with intensity maxima along lines with an angle $\theta/2$ as described in [14]. In other words, a spatial interference pattern of the form $\cos[k_g(x-z\theta/2)]$ with the wave number $k_g = 2\pi/d$ will be observed. If the $n=0, 1$ paths depicted in Fig. 1 are regarded as plane waves interfering at an angle $\theta = \lambda_{dB} d^{-1}$ then by geometry an effective phase shift

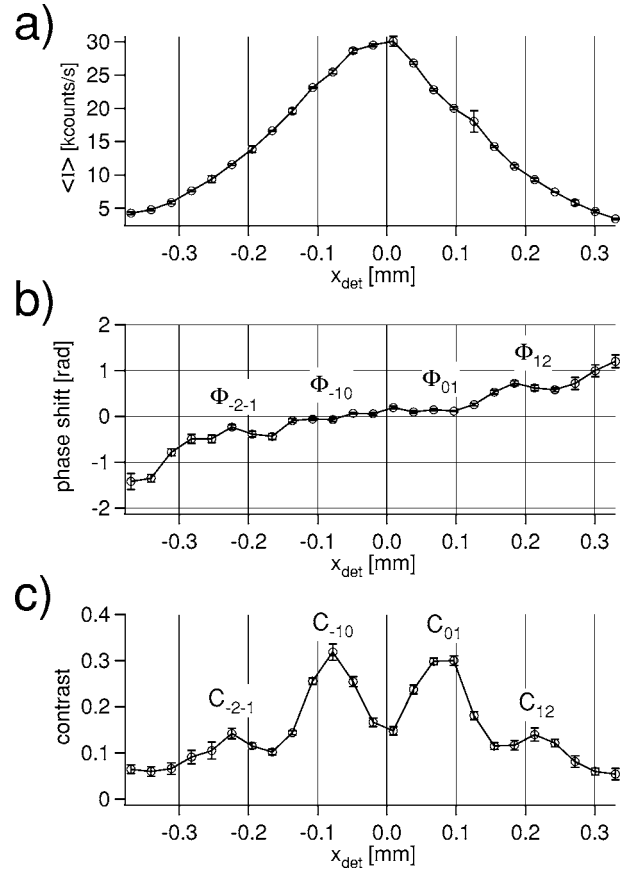


FIG. 2. Measured average intensity (a), phase (b), and contrast (c) as a function of detector position. The contrast C_{mn} and phase Φ_{mn} of a given interferometer output are defined in Eqs. (8) and (9). From the contrast profile one can clearly make out the different interferometer outputs as indicated in Fig. 1. The grating distance mismatch ΔL was chosen so that $\Phi_{01} = -\Phi_{-10} \approx 0$.

$$\Phi_{\Delta L} = \frac{\pi \Delta L \lambda_{dB}}{d^2}, \quad (4)$$

will be observed if there is a distance mismatch $\Delta L \equiv L'' - L'$ between the interferometer gratings. For two general paths originating from the diffraction orders m, n of G_1 the effective phase shift induced by ΔL will be given by $(m+n)\Phi_{\Delta L}$, since the fringe maxima are just rotated by an angle $(m+n)\theta/2$ with respect to the z axis.

The expressions for the diffraction phase Φ_n [Eq. (1)] and grating distance mismatch phase $\Phi_{\Delta L}$ [Eq. (4)] can then be used to specify the wave function $|\chi_{mn}\rangle$ just before the grating G_3

$$|\chi_{mn}\rangle = e^{ik_s x} |\psi_m\rangle + e^{i(m+n)\Phi_{\Delta L}} |\psi_n\rangle, \quad (5)$$

for any two interfering paths involving the diffraction orders m, n of grating G_1 . The wave functions $|\psi_m\rangle$ and $|\psi_n\rangle$ describe the two atom beams corresponding to a given interferometer output and accounts for the diffraction phases and amplitudes through the relations

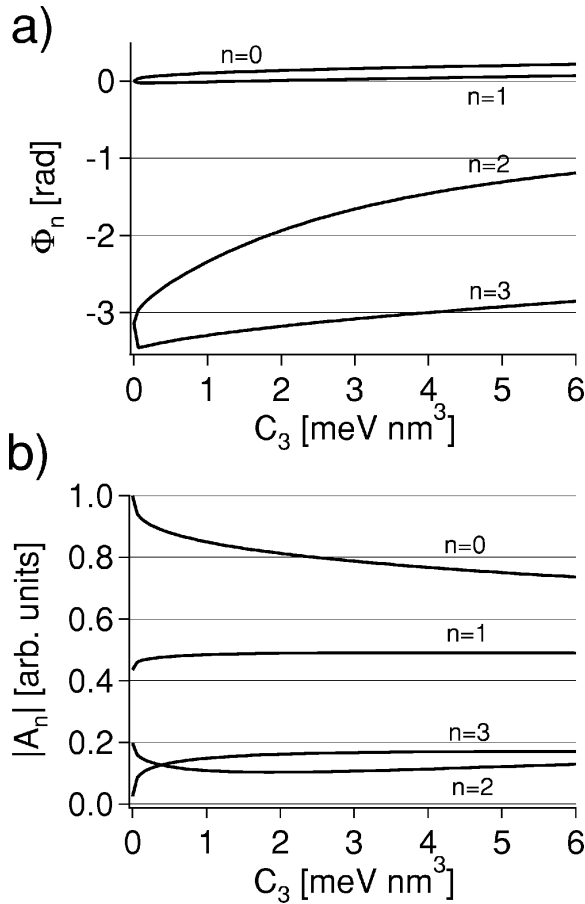


FIG. 3. Plots of the diffraction phases Φ_n (a) and amplitudes A_n (b) as a function of the vdW coefficient C_3 for diffraction orders $n=0, 1, 2, 3$ according to Eq. (1). The grating parameters $w=65$ nm, $l=150$ nm, $d=100$ nm, and atom beam velocity $v=2900$ m/s were used to generate the curves.

$$\langle \psi_n | \psi_n \rangle \equiv |A_n|^2, \quad (6)$$

and

$$\langle \psi_n | \psi_m \rangle \equiv A_n^* A_m e^{i(\Phi_m - \Phi_n)}, \quad (7)$$

where A_m , A_n and Φ_m , Φ_n are given by Eq. (1). The intensity can then be found in the usual way

$$I_{mn}(x) \equiv \langle \chi_{mn} | \chi_{mn} \rangle \propto 1 + C_{mn} \cos(k_g x + \Phi_{mn}), \quad (8)$$

where C_{mn} and Φ_{mn} are the observed contrast and phase for a given interferometer output involving the diffraction orders m, n as depicted in Fig. 1. The measured interferometer phase

$$\Phi_{mn} \equiv (\Phi_m - \Phi_n) - (m + n)\Phi_{\Delta L} \quad (9)$$

can also be expressed in terms of the diffraction phases Φ_n and grating mismatch phase shift $\Phi_{\Delta L}$. From Eq. (9) it can be seen that $\Phi_{mn} = -\Phi_{-n-m}$, as implied by the symmetry of the interferometers.

Equations (8) and (9) can now be used to predict the phase shift between the various interferometer outputs shown in Fig. 1. One noteworthy aspect of Eq. (9) is the possibility for Φ_{mn} to be made zero if the diffraction phase term is

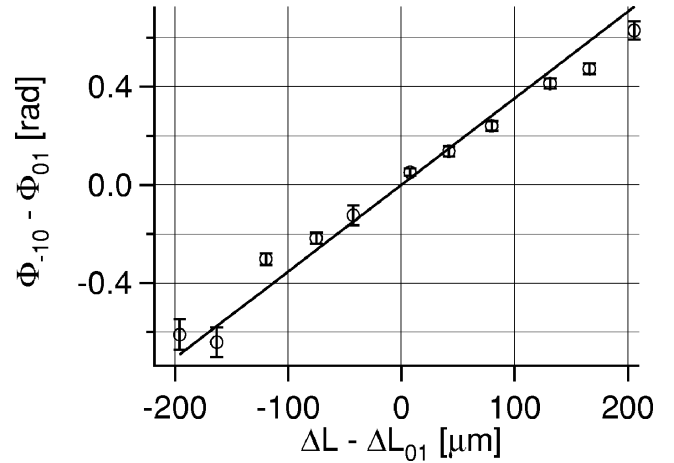


FIG. 4. Measured phase difference as a function of ΔL . The variable ΔL_{01} is the grating distance mismatch required to make the observed phase difference zero. The solid line contains no free parameters and is the phase difference implied by Eqs. (4) and (9) for the independently measured velocity $v=2900$ m/s ($\lambda_{dB}=0.056$ Å) and $d=100$ nm.

cancelled by an appropriate choice of ΔL . To verify this prediction the phase difference $\Phi_{-10} - \Phi_{01} = -2\Phi_{01}$ was measured as a function of ΔL and the results are shown in Fig. 4. The atom beam velocity $v=2900$ m/s ($\lambda_{dB}=0.056$ Å) was measured independently by observing the diffraction pattern generated by G_1 when the other gratings are removed. Equations (4) and (9) can then be used to generate the solid line in Fig. 4, since the grating period is known to be $d=100$ nm. The data agree quite well with our theory considering that there are no free parameters in the solid line. At this point ΔL is known only up to some offset ΔL_{01} which can be interpreted as the grating distance mismatch which leads to the special case of $\Phi_{\Delta L} = \Phi_0 - \Phi_1$. However, the value of ΔL_{01} will be determined next using another independent measurement technique.

As ΔL is shifted further from zero the partial spatial and temporal coherence of the atom beam causes the measured interference contrast to decrease. This notion is evident in the experimental data presented in Fig. 5, which plots the observed interference contrast as a function of ΔL . This phenomenon can be used to determine the offset ΔL_{01} , which then specifies the value of $\Phi_0 - \Phi_1$ through Eqs. (4) and (9).

The temporal coherence of the atom beam is determined by the wavelength, or equivalently the velocity, distribution of the atoms which make up the atom beam. As implied by Eq. (4), each wavelength component of the distribution will have a different phase shift for a given ΔL , leading to a reduction in contrast. If the wavelength is normally distributed with variance σ_λ^2 , then the nominal contrast C_o will be modified according to

$$C = C_o \exp \left[-\frac{1}{2} \left(\frac{\pi \sigma_\lambda \Delta L}{d^2} \right)^2 \right], \quad (10)$$

where the interference patterns corresponding to the fluctuations $\Delta \lambda$ about the mean have been summed over.

The spatial coherence of the atom beam is determined by

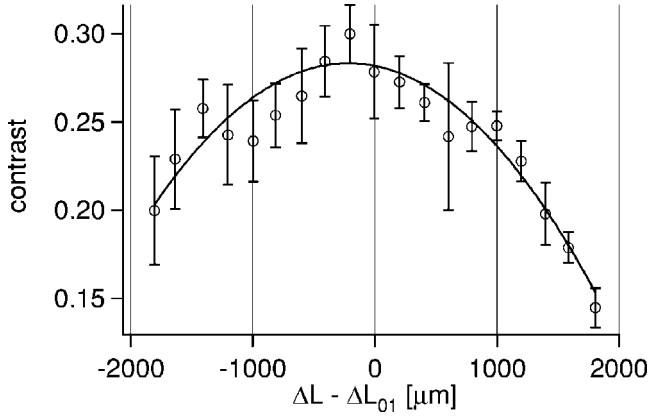


FIG. 5. Measured contrast as a function of the grating distance mismatch ΔL . The solid curve is a best fit parabola, which led to the determination of $\Delta L_{01} = 218 \pm 72 \mu\text{m}$.

the spatial extent of the atom beam source, and describes the correlation of different transverse points of the wave function. Since $\theta = \lambda_{dB} d^{-1} \approx 60 \mu\text{rad}$, when $\Delta L = 1 \text{ mm}$ there is about 60 nm of shear (i.e., transverse displacement) of the two interfering beams. As a result the contrast will be reduced because the regions of overlap for the two interfering wave functions will be less correlated when there is nonzero shear. The van Cittert–Zernike theorem states that the contrast will be reduced in a way that is related to the spatial Fourier transform of the atom beam source profile [6]. If the source intensity distribution is assumed to be $w_c^{-1} \text{rect}(xw_c^{-1})$, given that $\text{rect}(\arg) = 1$ when $|\arg| \leq 1/2$ and zero otherwise, then the contrast will be reduced according to

$$C = C_o \left| \text{sinc} \left(\frac{w_c s}{\lambda_{dB} z_c} \right) \right| = C_o \left| \text{sinc} \left(\frac{w_c \Delta L}{dz_c} \right) \right|, \quad (11)$$

where w_c is the collimation slit width, z_c is the distance from the collimation slit to G_3 , and $s = \Delta L \theta$ is the amount of induced shear. Both Eqs. (10) and (11) are similar to ones found in [15] derived using a different method.

Near $\Delta L = 0$ Eqs. (10) and (11) are approximately parabolic so a quadratic $C = C_o [1 - a(\Delta L - \Delta L_{01})^2]$ was fit to the data in Fig. 5 to determine the offset $\Delta L_{01} = 218 \pm 72 \mu\text{m}$ and curvature $a = 0.11 \pm 0.01 \text{ mm}^{-2}$. The best fit curvature of the parabola implies a wavelength spread of $\sigma_\lambda = 0.015 \text{ \AA}$ according to Eq. (10), which is considerably larger than $\sigma_\lambda = 0.006 \text{ \AA}$ obtained from the diffraction pattern of G_1 alone. However, a collimation slit width of $w_c = 73 \mu\text{m}$ with $z_c = 2.8 \text{ m}$ is consistent with the curvature of the parabola, according to Eq. (11). When simultaneously considering the effects of temporal *and* spatial coherence, the contrast will be proportional to the product of Eqs. (10) and (11). With this in mind, the independently measured value for $\sigma_\lambda = 0.006 \text{ \AA}$ and the curvature of the parabola yields only a slightly smaller collimation slit width of $w_c = 67 \mu\text{m}$. Therefore, the observed reduction in contrast as a function of ΔL is most likely dominated by spatial coherence effects.

Given the data in Figs. 4 and 5 the best fit value of ΔL_{01} implies that $\Phi_0 - \Phi_1 = 0.39 \pm 0.13 \text{ rad}$, according to Eq. (4).

TABLE I. Measured and calculated values of Φ_n .

n	Measured Φ_n (rad)	Predicted ^b Φ_n (rad)
0	0.30 ± 0.15^a	0.16
1	-0.09 ± 0.20	0.02
2	-1.66 ± 0.48	-1.71

^aThe value was measured in [11].

^bValues are calculated with Eq. (1) and $C_3 = 2.7 \text{ meV nm}^3$ for Na atoms and a silicon nitride surface [5].

The diffraction phase $\Phi_0 = 0.30 \pm 0.15 \text{ rad}$ was measured recently in [11], which yields the first order diffraction phase $\Phi_1 = -0.09 \pm 0.20 \text{ rad}$. This value for Φ_1 is consistent with the value predicted by Eq. (1), as summarized in Table I.

By moving the detector so that it intercepts the different interferometer outputs indicated in Fig. 1 the higher order diffraction phases can be determined. The measured contrast, phase, and intensity are shown in Fig. 2 as a function of detector position. From Fig. 2 the phase $\Phi_{12} = 0.4 \pm 0.2 \text{ rad}$ can be determined. Equation (9) then implies that $\Phi_1 - \Phi_2 = 1.57 \pm 0.44 \text{ rad}$, which finally leads to $\Phi_2 = -1.66 \pm 0.48 \text{ rad}$. This value compares well to that predicted by Eq. (1), as shown in Table I.

Based on the predictions in Fig. 3 and Eq. (1), the measured value of Φ_2 is best described when $C_3 = 3_{-1.5}^{+3} \text{ meV nm}^3$ (statistical), which is not yet competitive with the $\sim 30\%$ uncertainty of other methods [5,11,16]. In principle, this uncertainty could be reduced by making σ_λ or w_c larger so that $C(\Delta L)$ in Eqs. (10) and (11) is more sharply peaked, leading to a smaller uncertainty in ΔL_{01} . From the predictions in Fig. 3 and Eq. (2) one can also see that C_3 is less sensitive to changes in Φ_2 for larger v (or smaller C_3). Therefore, using atoms with a smaller polarizability (e.g., He) or larger velocity could reduce the measurement uncertainty in C_3 for this method. However, these improvements can also result in broader beams and overlapping interferometer outputs, leading to a practical tradeoff between uncertainty in Φ_{mn} and ΔL_{01} . Unfortunately, the diffraction phase Φ_1 has a very weak dependence on C_3 , as evident in Fig. 3, and is less useful for measuring the vdW coefficient compared to Φ_2 .

In conclusion the atomic diffraction phases Φ_n induced by a material grating structure have been measured for $n = 0, 1, 2$. This was accomplished by comparing the relative phases of the various outputs of a three-grating Mach-Zehnder atom interferometer. These measurements agree with a simple model that includes a vdW atom-surface interaction between the Na atom beam and the silicon nitride grating. In the future, one could simultaneously monitor Φ_{01} and Φ_{-10} with two detectors, while applying some interaction to the $n=1$ arm. One could then perform self-referencing phase measurements with the interferometer, eliminating the need to take control data in a serial fashion. In this type of application knowledge of the diffraction phases observed here would be required.

This work was supported by Research Corporation and the National Science Foundation under Grant No. 0354947.

- [1] *Atom Interferometry*, edited by P. R. Berman (Academic Press, New York, 1997).
- [2] M. Weitz, B. C. Young, and S. Chu, *Phys. Rev. A* **50**, 2438 (1994).
- [3] S. Durr, T. Nonn, and G. Rempe, *Nature (London)* **395**, 33 (1998).
- [4] M. Buchner, R. Delhulle, A. Miffre, C. Robilliard, J. Vigue, and C. Champenois, *Phys. Rev. A* **68**, 013607 (2003).
- [5] J. D. Perreault, A. D. Cronin, and T. A. Savas, *Phys. Rev. A* **71**, 053612 (2005).
- [6] M. Born and E. Wolf, *Principles of Optics* (Cambridge University Press, Cambridge, 1999).
- [7] T. L. Gustavson, A. Landragin, and M. A. Kasevich, *Class. Quantum Grav.* **17**, 2385 (2000).
- [8] P. W. Milonni, *The Quantum Vacuum* (Academic Press, New York, 1994).
- [9] R. E. Grisenti, W. Schollkopf, J. P. Toennies, G. C. Hergerfeldt, and T. Kohler, *Phys. Rev. Lett.* **83**, 1755 (1999).
- [10] A. D. Cronin and J. D. Perreault, *Phys. Rev. A* **70**, 043607 (2004).
- [11] J. D. Perreault and A. D. Cronin, *Phys. Rev. Lett.* **95**, 133201 (2005).
- [12] D. W. Keith, C. R. Ekstrom, Q. A. Turchette, and D. E. Pritchard, *Phys. Rev. Lett.* **66**, 2693 (1991).
- [13] T. A. Savas, M. L. Schattenburg, J. M. Carter, and H. I. Smith, *J. Vac. Sci. Technol. B* **14**, 4167 (1996).
- [14] E. Hecht, *Optics* (Addison-Wesley, Reading, MA, 1998).
- [15] C. Champenois, M. Buchner, and J. Vigue, *Eur. Phys. J. D* **5**, 363 (1999).
- [16] A. Landragin, J. Y. Courtois, G. Labeyrie, N. Vansteenkiste, C. I. Westbrook, and A. Aspect, *Phys. Rev. Lett.* **77**, 1464 (1996).